ADVANCED FUNCTIONAL MATERIALS
www.afm-journal.de

Excited State Dynamics of a Self-Doped Conjugated Polyelectrolyte

*Demetra Tsokkou, Lisa Peterhans, David Xi Cao, Cheng-Kang Mai, Guillermo C. Bazan, Thuc-Quyen Nguyen, and Natalie Banerji**

The growing number of applications of doped organic semiconductors drives the development of highly conductive and stable materials. Lack of understanding about the formation and properties of mobile charges limits the ability to improve material design. Thus the largely unexplored photophysics of doped systems are addressed here to gain insights about the characteristics of doping-induced polarons and their interactions with their surroundings. The study of the ultrafast optical processes in a self-doped conjugated polyelectrolyte reveals that polarons not only affect their environment via Coulomb effects but also strongly couple electronically to nearby neutral sites. This is unambiguously demonstrated by the simultaneous depletion of both the neutral and polaronic transitions, as well as by correlated excited state dynamics, when either transition is targeted during ultrafast experiments. The results contrast with the conventional picture of localized intragap polaron states but agree with revised models for the optical transitions in doped organic materials, which predict a common ground level for polarons and neighboring neutral sites. Such delocalization of polarons into the frontier transport levels of their surroundings could enhance the electronic connectivity between doped and undoped sites, contributing to the formation of conductive charges.

1. Introduction

Doping of organic semiconductors is required to achieve high conductivities. Significant efforts have thus been invested to understand and to improve the electrical and transport properties of doped organic semiconductors through understanding of the elementary processes associated with different levels and types of doping.[1] Experimental and theoretical research on doped organic semiconductors has been intensified over the past few years as a consequence of recent synthetic advances that enable better control over the bulk distribution and stability of charges.[2–5] One drawback in the field is that upon doping of organic semiconductors, even for systems where integer charge transfer occurs between the dopant and the host, only a small fraction (typically 5%) of the charges are mobile and contribute to the conductivity, while most of them remain bound to the ionized dopant.[6,7] It is therefore essential to gain deep insights about the optoelectronic properties of doping-induced charges, in order to understand the parameters that govern their dissociation from the dopant. Ultrafast spectroscopy, which has already been extensively used to address the related question of interfacial charge separation in organic photovoltaics,[7,8] provides a powerful but still unexploited tool to investigate charges in doped systems. Here, we experimentally study the ultrafast photophysical properties of a self-doped conjugated polyelectrolyte (CPE). Using transient absorption (TA) spectroscopy, we shed light on optoelectronic properties of doping-induced polarons and their interactions with their surroundings.

CPEs are composed of a π-conjugated backbone and ionic functionalities on the side chains that increase solubility in polar solvents. The latter extends the applications of CPEs from organic electronics to biosensing and bioimaging.[9] In this work, a solution-processed narrow-bandgap CPE with a π-conjugated cyclopenta-[2,1-b;3,4-b′]-dithiophene-alt-4,7-(2,1,3-benzothiadiazole) (PCPDTBT) backbone, and sulfonated side chains (CPE-K, inset of **Figure 1**a) is investigated. Upon dialysis treatment in water, CPE-K forms cationic polarons, presumably initiated via protonation of the backbone followed by electron transfer from a neutral chain, becoming self-doped.[2,10,11] The negatively charged sulfonate side chains counterbalance the positive charges on the conjugated backbone without need for external dopants. Because of the large increase in bulk conductivity upon doping, CPE-K has been used as hole transport material for organic and perovskite solar cells with comparable performance to widely used and commercially available poly(3,4-ethylenedioxythiophene):poly(styrenesulfonate) (PEDOT:PSS).[12,13] Self-doped CPE-K shows important benefits compared to externally doped systems, such as absence of dopant diffusion (unlike with

Dr. D. Tsokkou, Dr. L. Peterhans, Prof. N. Banerji
Department of Chemistry and Biochemistry
University of Bern
Freiestrasse 3, 3012 Bern, Switzerland
E-mail: natalie.banerji@dcb.unibe.ch
D. X. Cao, Dr. C.-K. Mai, Prof. G. C. Bazan, Prof. T.-Q. Nguyen
Center for Polymers and Organic Solids
Department of Chemistry and Biochemistry
University of California
Santa Barbara, CA 93106, USA
The ORCID identification number(s) for the author(s) of this article can be found under https://doi.org/10.1002/adfm.201906148.

DOI: 10.1002/adfm.201906148

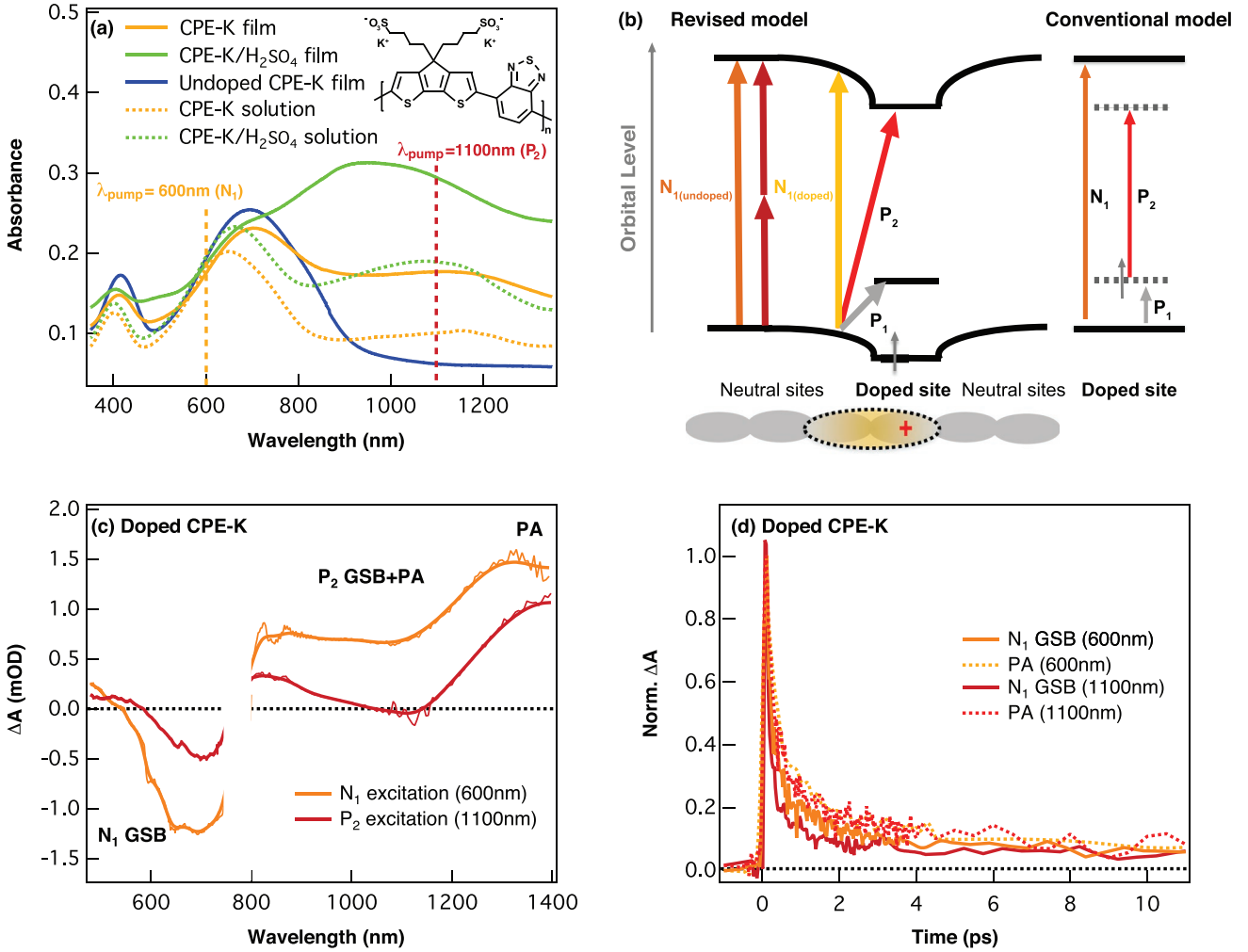

Figure 1. Optical transitions in doped CPE-K. a) Steady-state absorption spectra of doped CPE-K, doped CPE-K/H_2SO_4 and undoped CPE-K films and solutions. The excitation wavelengths used in transient absorption (TA) measurements are indicated as vertical orange (600 nm, visible) and dark red (1100 nm, near-infrared) dotted lines, where photoexcitation is resonant with the N_1 and P_2 transitions, respectively. The inset shows the molecular structure of CPE-K. b) On the left, the recently proposed energy level diagram for doped conjugated systems and the corresponding origin of the optical N_1 and P_2 transitions are shown with solid arrows.[17] On the right side, the energy levels and optical transitions based on the conventional model (not in agreement with our experimental data) are shown. c) TA spectra at an early time delay (0.1 ps) of doped CPE-K at a similar absorbed photon density of ≈1.5×10^{13} cm^{-2} for 600 and 1100 nm excitation. Comparable spectral signatures including the N_1 GSB (ground state bleaching of N_1 transition), P_2 GSB (ground state bleaching of P_2 transition), and PA (photoinduced absorption) are seen. d) Temporal evolution of the normalized dynamics probed at the N_1 GSB and PA band maxima for doped CPE-K with 600 and 1100 nm excitation at low absorbed photon density (≈1.5×10^{13} cm^{-2}).

small external dopant molecules),[14] less morphological disruption of the films (while doping with F_4TCNQ typically deteriorates the film quality),[15] and no hybridization of the host and dopant orbitals (in contrast to PCPDTBT:F_4-TCNQ blends.)[5,16]

Our results with films and dissolved CPE-K systems provide the first experimental evidence that the polaronic sites do not only provoke Coulomb interactions with their surroundings, but also strongly couple electronically to nearby neutral sites of the conjugated backbone. This is consistent with recent electronic structure models of doped organic semiconductors,[5,17–19] but cannot be explained within the conventional picture.[20,21] In the conventional model, the introduction of polarons induces localized intragap states, while the energy levels of the neutral sites remain unaffected. In contrast, the revised models include modifications to the electronic structure and optical transitions caused by interactions of the polarons with their environment, as discussed in detail later on. Here, we experimentally evidence delocalization of the polarons into the frontier transport levels of their surroundings, which enhances the electronic connectivity between doped and undoped sites and might contribute to the formation of conductive charges in doped conjugated systems.

2. Results and Discussion

2.1. Optical Transitions in the Doped Materials

The absorption spectra of doped CPE-K, heavily doped CPE-K (achieved upon H_2SO_4 treatment) and undoped CPE-K are

shown in Figure 1a (films and solutions). All systems exhibit two main absorption bands at wavelengths shorter than 900 nm, similar to the PCPDTBT polymer without ionic side chains.[22] The main visible (vis) absorption band peaking at ≈703 nm (in the films) is associated to the S_0–S_1 transitions of neutral (undoped) sites, which we will refer to as N_1 transition for simplicity. In the doped systems, an additional band in the near-infrared (NIR) is evident in the wavelength range studied here, related to the P_2 transition due to cationic polarons on the backbone.[2,10,11] The intensity of the P_2 band increases with the addition of acid, which is indicative that the polaron concentration is higher in CPE-K/H_2SO_4. This is further supported by electron paramagnetic resonance (EPR) measurements that we have previously reported.[11] The EPR signal scales with the polaron concentration and strength of the P_2 absorption band, so that a higher EPR signal is measured after the acid treatment. Also, the dc conductivity of 3×10^{-2} S cm^{-1} for doped CPE-K film significantly increases after the addition of H_2SO_4 (1.4×10^{-1} S cm^{-1}), due to the higher doping level, which affects both the number and mobility of the conductive charges.[23] To obtain quantitative doping concentrations, we have determined the absorption cross-section of the P_2 polaron band from TA measurements on photoexcited PCPDTBT:fullerene films (Figure S1, Supporting Information). From this, we find a polaron concentration of 1.5×10^{20} cm^{-3} in doped CPE-K film and of 2.4×10^{20} cm^{-3} in doped CPE-K/H_2SO_4 film, based on the intensity of their P_2 absorption bands (see details in the Supporting Information). This means that respectively ≈17% and ≈27% of monomers are charged, which, for an average chain length of 7–14 monomers as used here, corresponds to 1–2 charged monomers per chain in CPE-K and 2–3 charged monomers per chain in CPE-K/H_2SO_4. Some de-doping occurs during dissolution, so that we find that only 8% and 14% of monomers are charged in doped CPE-K and CPE-K/H_2SO_4 solution, respectively (Figure S2, Supporting Information).

In general, the presence of polarons on the conjugated backbone leads to the emergence of new characteristic absorption bands at energies below the bandgap of the neutral semiconductor,[20,24] associated with the P_2 and P_1 transitions. The consensus is that the addition/extraction of electrons from the neutral semiconductor introduces intragap localized energy levels, due to local nuclear reorganization of the doped site (usually from a benzoid to a more quinoid structure), while the energy levels of the neutral sites remain unaffected.[20,21] For cationic polarons, it is stipulated that a singly occupied energy level located above the highest occupied molecular orbital (HOMO) level and an unoccupied energy level below the lowest unoccupied molecular orbital (LUMO) level of the neutral semiconductor are formed and that the polaronic P_2 transition occurs between localized intragap levels, while the P_1 transition takes place between the HOMO and the singly occupied level, as shown on the right of Figure 1b.[20,21] This approach neglects electron–electron interactions on the polaronic site and with neighboring neutral sites, so that modifications to the conventional model have recently been proposed (left of Figure 1b).[5,17–19] Due to on-site Coulomb repulsions, the lower intergap polaronic level splits so that the lone electron level is located below the HOMO level of the neutral organic semiconductor, and both the frontier energy levels are stabilized on the doped site. Moreover, intersite Coulomb interactions down-shift the energy levels of neutral sites located near the positive charge. Within this framework and according to time-dependent density functional theory (TD-DFT) calculations on doped poly-(para-phenylene), the P_2 band is assigned to a charge transfer type transition from the HOMO level of neutral sites adjacent to the polaron to the unoccupied intragap level of the polaronic site.[17] This is in contrast to the intergap P_2 transition predicted by the conventional model. The N_1 transition, however, occurs between the HOMO and LUMO levels of the neutral sites in both approaches. Lastly, the P_1 transition involves the HOMO of the neutral sites to the unoccupied level of the doped sites (new model) but will not be discussed further since it is out of the spectral range accessible by our TA measurements.

For the purpose of this study, TA measurements were performed at different excitation wavelengths by selectively pumping the N_1 transition at 600 nm or the P_2 transition at 1100 nm (vertical dotted lines in Figure 1a). The early TA spectra, recorded 0.1 ps after photoexcitation of doped CPE-K film, are compared for the two excitation wavelengths in Figure 1c and have surprisingly similar features. Both show a negative signal attributed to ground state bleaching of the N_1 transition (N_1 GSB) at vis wavelengths, a broad positive band related to photoinduced absorption (PA) at NIR wavelengths, and an overlapping negative band in the NIR that we assign to the GSB of the P_2 transition (P_2 GSB), as it matches the polaron absorption band. This is surprising, since it unambiguously shows that both 600 and 1100 nm excitation result in simultaneous depletion of the N_1 and P_2 transitions, within the ≈70 fs time resolution of our experiment. Moreover, the excited state dynamics, probed either in the N_1 GSB or overlapping P_2 GSB/PA band, is also comparable for both excitation wavelengths (Figure 1d).

This finding is in disagreement with the conventional description of the transitions for doped organic semiconductors (right of Figure 1b), since here the N_1 and P_2 transitions involve completely independent energy levels.[20,21] According to the conventional model, resonant excitation of the N_1 transition should lead to only the N_1 GSB and PA features similar as observed in undoped CPE-K (see below), while photoexcitation of the P_2 transition should lead to signatures of the P_2 GSB and of photoexcited polarons, having independent relaxation dynamics compared to the N_1 excited state. The observed GSB signatures of both the N_1 and P_2 transitions could in principle result from excited state charge transfer processes between the doped and neutral sites. However, we see no experimental evidence resolving such a behavior upon excitation of either transition, since both GSB features appear already within the ≈70 fs time resolution of the experiment for both excitation wavelengths. This points to strong coupling between the doped and adjacent neutral sites, so that ultrafast charge transfer likely occurs directly upon excitation (without locally excited intermediate). We note that this interpretation is equivalent to the assignment of the P_2 band as a transition from the HOMO level of a neutral site to the unoccupied intragap level of the polaronic site, as predicted by the TD-DFT calculations on doped poly-(para-phenylene) and shown on the left of Figure 1b.[17] This revised model is also in excellent agreement with the depletion of the P_2 transition when exciting the N_1 band at 600 nm. Since the N_1 transition (of neutral sites adjacent to the polaron) has the same ground level as the P_2 transition, simultaneous depletion and recovery when exciting in either absorption band

is expected, implying that there is strong electronic coupling between doped and nearby undoped sites.

2.2. N_1 Excitation of Doped and Undoped CPE-K Films

In order to further substantiate this finding, we now turn to the details of the TA data. **Figure 2** presents the TA results for undoped and doped CPE-K films via 600 nm excitation, where the N_1 transition is resonantly pumped. The TA spectra of undoped CPE-K (Figure 2a) show a similar behavior as reported for the undoped PCPDTBT polymer.[25] A negative signal attributed to the N_1 GSB is observed at vis wavelengths and its normalized TA dynamics is included in Figure 2b. In addition, a broad positive PA band by the S_1 excited state is seen at NIR wavelengths. The TA spectra obtained in doped CPE-K at selected time delays are displayed in Figure 2c. Similar to undoped CPE-K, the N_1 GSB and PA bands are evident and thus are related to population of the S_1 state via the N_1 transition. As mentioned above, an additional dip is seen in the PA band at very early times (≈0.1 ps), caused by its overlap with the P_2 GSB that quickly disappears. We associate the fact that 600 nm excitation results in simultaneous depletion of the N_1 and P_2 transitions to delocalization of the involved electronic states over both doped and neutral sites due to strong electronic coupling, so that the N_1 and P_2 transitions share the same ground level (left of Figure 1b). Since the high energy part of the N_1 band is photoexcited at 600 nm, it is unlikely that our observations arise from direct excitation of the P_2 band tail and we provide further evidence below to exclude this.

Another consequence of doping is the significantly faster excited state decay in doped CPE-K compared to undoped CPE-K (Figure 2b). Most photoexcitations recombine within one picosecond in the doped film, as shown by the dynamics probed in both the N_1 GSB and PA bands, while only about half of the photoexcitations recombine in undoped CPE-K within the first 5 ps. The faster recombination in doped CPE-K is consistent with the decrease in photoluminescence yield and lifetime upon the addition of charges in organic systems.[26] To distinguish between spectral components that decay with different times constants, we have analyzed the entire spectral and temporal pump-probe datasets using multiexponential global analysis (GA). The amplitude spectra associated with each of the time constants for doped CPE-K are shown in Figure 2d. The dominant recombination component is ultrafast with a time constant of ≈150 fs and involves both the N_1 and P_2 GSB bands. It is absent in undoped CPE-K (Figure S3, Supporting Information). The simultaneous ground state recovery in this component is further evidence that the N_1 and P_2 transitions are coupled and that our results do not arise from their uncorrelated excitation. As further elaborated later on, we assign the ultrafast (≈150 fs) recombination to polymer segments that contain a polaronic site (referred to as "doped chromophores"), where the neutral sites excited at 600 nm are coupled to the close-by polaron (transition $N_{1(doped)}$ in Figure 1b). On the other hand, the weak amplitude spectra related to the slower time

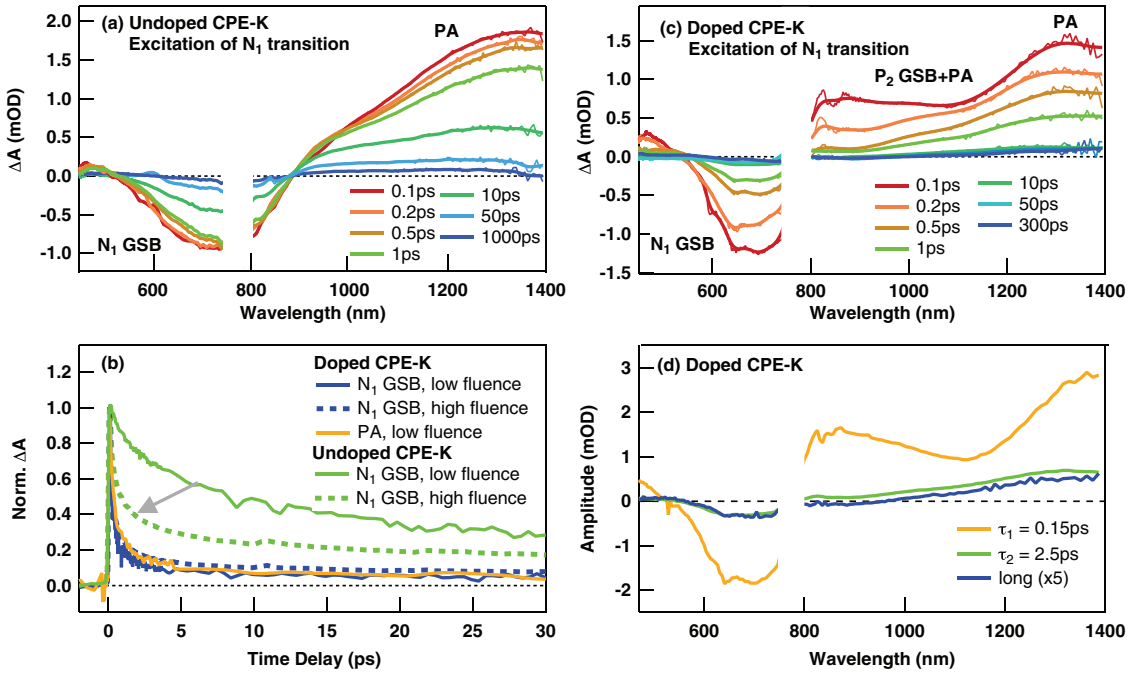

Figure 2. Transient absorption (TA) results for visible excitation (at 600 nm) of the N_1 transition of undoped and doped CPE-K films. TA spectra at selected time delays of a) undoped CPE-K at an absorbed photon density of ≈5×10^{12} cm^{-2} and c) doped CPE-K at an absorbed photon density of ≈1.5×10^{13} cm^{-2}. b) Temporal evolution of the normalized dynamics in doped CPE-K probed at the N_1 GSB (visible ground state bleaching) and PA (photoinduced absorption) band maxima and in undoped CPE-K probed at the N_1 GSB band maximum. Dynamics for low absorbed photon density (≈5×10^{12} cm^{-2}, solid lines) and high absorbed photon density (≈2.2×10^{14} cm^{-2}, dotted lines) are included. d) Amplitude spectra associated with the different recombination time constants (0.15, 2.5 ps and long-lived offset) in doped CPE-K, as derived from multiexponential global analysis of the TA data at an absorbed photon density of ≈1.5×10^{13} cm^{-2}.

constants (≈2.5 ps and long (>>1 ns)) are similar to the TA spectra of undoped CPE-K (Figure 2a) and do not involve the P_2 GSB. We attribute those to neutral polymer segments located further away or not conjugated to the polaronic site and thus not electronically coupling to it ("undoped chromophores," $N_{1(undoped)}$ transition). We note the relatively small amplitude of the 2.5 ps component compared to the 150 fs component (Figure 2d), which indicates that most neutral sites in doped CPE-K couple to polarons. Indeed, based on the intensity of the N_1 GSB in the 150 fs amplitude spectrum compared to the longer recombination components, we estimate that 83% of the neutral monomers couple to a polaronic site (**Table 1**). This can be explained by the high doping level and the delocalization of photoexcited chromophores in doped CPE-K films.

Finally, we also note a difference in the behavior of doped and undoped CPE-K during intensity-dependent TA measurements (Figure 2b). As expected, in undoped CPE-K film, exciton–exciton annihilation becomes significant as the absorbed photon density increases, leading to faster recombination dynamics.[27] In contrast, the dynamics in doped CPE-K is unchanged even at high absorbed photon densities (≈2.2×10^{14} cm^{-2}), showing that the presence of polarons prevails this process. Due to the large spectral overlap between the exciton emission spectrum and polaron absorption spectrum, exciton-polaron annihilation is intrinsically more efficient than exciton–exciton annihilation in photoexcited polymer:fullerene blends.[28] Therefore, it is expected to become important in doped systems at high polaron concentrations. Thus, exciton-polaron annihilation for

Table 1. Position of the N_1 and P_2 steady-state absorption bands of the doped CPE-K and CPE-K/H_2SO_4 films and solutions, together with the position and amplitude of the N_1 ground state bleaching (GSB) band in the amplitude spectra (corresponding to the τ_1-τ_3 time constants) obtained from the global analysis (GA) of the transient absorption data. The ratio of the N_1/P_2 amplitudes is then related to the concentration of doped monomers (expressed as a % and as a ratio of neutral to doped monomers). All data were collected at similar absorbed photon density.

		N_1 band position (±5 nm in GA) [nm]	P_2 band position [nm]	N_1 GSB amplitude [mOD]	N_1/P_2 band amplitudes	% of doped monomers	Ratio neutral to doped monomers
CPE-K film	**Steady-state**	703	1120		1.28	17	4.9:1
	GA (600 nm)						
	τ_1 = 0.15 ps	699		–1.84	0.97	23	3.3:1
	τ_2 = 2.5 ps (+long)	693		–0.38			
	GA (1100 nm)						
	τ_1 = 0.15 ps	705		–0.73	0.24	35	1.9:1
	τ_2 = 2.5 ps (+long)	689		–0.07			
CPE-K/H_2SO_4 film	**Steady-state**	703	950		0.77	27	2.7:1
	GA (600 nm)						
	τ_1 = 0.15 ps	661		–1.43	0.55	30	2.3:1
	τ_2 = 2.5 ps (+long)	656		–0.34			
	GA (1100 nm)						
	τ_1 = 0.15 ps	677		–0.58	0.18	36	1.8:1
	τ_2 = 2.5 ps (+long)	658		–0.08			
CPE-K solution	**Steady-state**	650	1150		2.00	8	11.5:1
	GA (600 nm)						
	τ_1 = 0.15 ps	704		–1.68	0.89	24	3.2:1
	τ_2 = 2 ps	702		–0.67			
	τ_3 = 40 ps	600		–0.90			
	GA (1100 nm)						
	τ_1 = 0.15 ps	699		–0.61	0.21	36	1.8:1
	τ_2 = 1.8 ps (+long)	699		–0.06			
CPE-K/H_2SO_4 solution	**Steady-state**	667	1080		1.21	14	6.1:1
	GA (600 nm)						
	τ_1 = 0.15 ps	662		–1.42	0.65	28	2.6:1
	τ_2 = 2.0 ps	662		–0.36			
	τ_3 = 40 ps	600		–0.30			
	GA (1100 nm)						
	τ_1 = 0.15 ps	660		–0.50	0.16	37	1.7:1
	τ_2 = 1.8 ps (+long)	676		–0.07			

undoped chromophores and ultrafast recombination in doped chromophores reduce the excitation density before any higher-order recombination effects take place, suppressing exciton–exciton annihilation.

2.3. P_2 Excitation of Doped CPE-K Films

To access directly the P_2 transition in doped CPE-K, we performed TA measurements using excitation of this band at 1100 nm. The TA spectra and GA results are displayed in **Figure 3**a,b, respectively. In the early TA spectra, the N_1 GSB band is present, while the NIR PA band overlaps with a more intense P_2 GSB band compared to that observed with 600 nm excitation. The simultaneous appearance of both the N_1 and P_2 GSB bands with P_2 excitation points again to coupling of the N_1 and P_2 transitions that share the same ground state, which strongly suggests electronic coupling between doped and nearby undoped sites, similarly to the results with 600 nm excitation. Nevertheless, to exclude that the N_1 GSB is related to direct excitation of undoped chromophores, we performed intensity-dependent TA measurements with 1100 nm excitation in doped and undoped CPE-K. As the pump photon energy is significantly lower than the undoped CPE-K energy gap, no resonant excitation should take place. Unexpectedly, we still observe similar TA spectral features and recombination dynamics for 1100 and 600 nm excitation in undoped CPE-K (Figure S4, Supporting Information). This behavior at 1100 nm can be explained by two-photon absorption (dark red arrows in Figure 1b), since the intensity of the early N_1 GSB (at 0.1 ps) in undoped CPE-K has a quadratic dependence on incident photon density (Figure 3c), similar as for PCPDTBT (Figure S5, Supporting Information). In contrast, the early N_1 GSB in doped CPE-K scales linearly with absorbed photon density (Figure 3c), confirming that this transition is not directly excited by two-photon absorption, but indirectly depleted via one-photon excitation of the P_2 band. Moreover, the difference in the photo excitation density between the two systems becomes evident when comparing the TA amplitudes for 1100 nm excitation. In undoped CPE-K, a pump fluence of at least one order of magnitude higher is needed to obtain a comparable N_1 GSB amplitude than in doped CPE-K.

In agreement with the strong coupling of the N_1 and P_2 transitions in doped CPE-K, similar fast recombination dynamics are obtained for both excitation of the N_1 transition at 600 nm and of the P_2 transition at 1100 nm (Figure 1d). The GA results for 1100 nm excitation (Figure 3b) confirm an ultrafast (≈150 fs) recombination component that includes both the N_1 and P_2

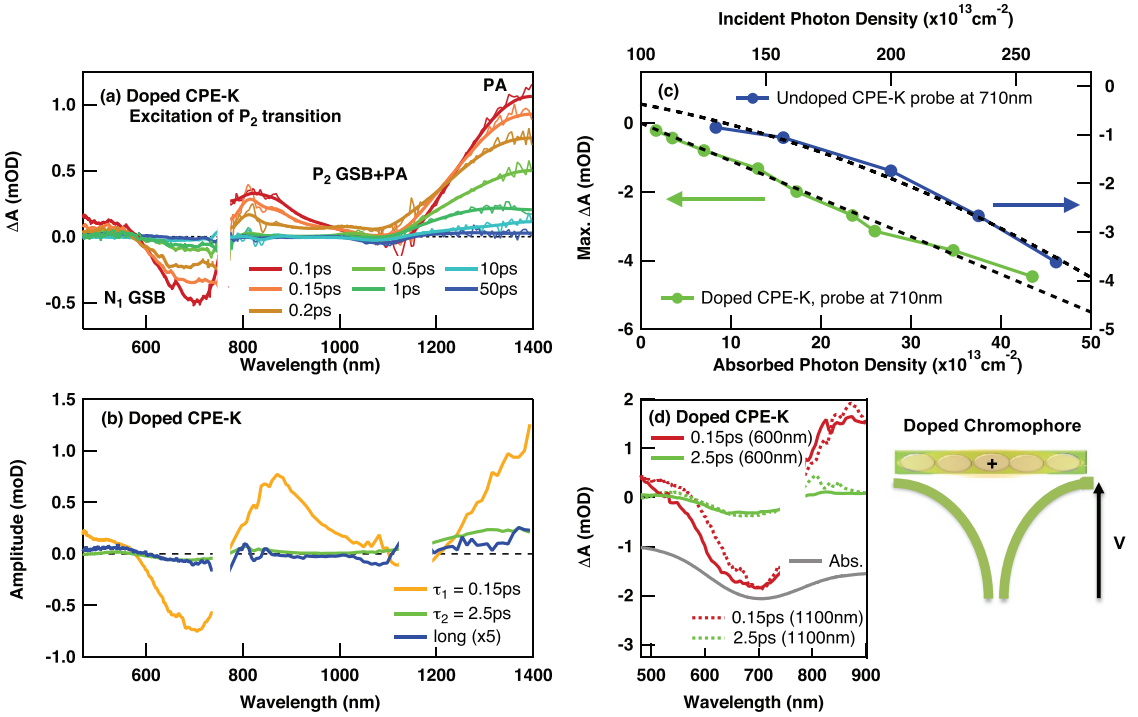

Figure 3. Transient absorption (TA) results for near-infrared excitation (at 1100 nm) of the P_2 transition of doped CPE-K film. a) TA spectra at selected time delays at an absorbed photon density of ≈1.5×10^{13} cm^{-2}. b) Amplitude spectra associated with the different recombination time constants (0.15, 2.5 ps, long-lived offset) as derived from multiexponential global analysis of the TA data at an absorbed photon density of ≈1.5×10^{13} cm^{-2}. c) Dependence of the initial TA signal intensity at 710 nm (N_1 GSB maximum, 0.1 ps after photoexcitation) as a function of photon density in doped CPE-K (left-bottom axes) and undoped CPE-K (top and right axes) excited at 1100 nm. d) Amplitude spectra in the visible region associated with the 0.15 ps time constant (red) and the 2.5 ps time constant (green) for CPE-K film excited at 600 nm (solid lines). Dotted lines show the respective amplitude spectra obtained with 1100 nm excitation, scaled to the same intensity. The absorption spectrum of the doped CPE-K film is shown for comparison. Also, a schematic representation of the polaron on a conjugated chain is included, which causes a Stark shift of the absorption of nearby neutral sites that are located within its Coulomb potential well.

GSB, as was observed with 600 nm excitation. We again assign this to ultrafast recombination in doped chromophores of CPE-K, which are directly excited at the polaronic site to the P_2 level. Such fast recombination of photoexcited polarons agrees with pump-push-probe experiments reported for photoexcited polymer:fullerene blends.[29] Given that the P_2 transition only excites doped chromophores, it is somewhat surprising that the slower decay components (≈2.5 ps and long) due to recombination of undoped chromophores are also present with 1100 nm excitation (although with five times weaker absolute amplitude compared to 600 nm excitation, Table 1). They are likely populated via residual two-photon absorption or by ultrafast localization of the initial photoexcitation onto neutral sites. Finally, we observe a less pronounced N_1 GSB with 1100 nm excitation compared to 600 nm excitation in the early TA spectra (Figure 1c, recorded at similar excitation density). This can be explained by two effects: the weaker population of undoped chromophores at 1100 nm and a reduced delocalization in the doped chromophores, containing fewer neutral sites. We have related the ratio of the N_1 to P_2 steady-state absorption bands to the concentration of doped monomers in Figure S6a in the Supporting Information. Comparing this to the ratio of the two corresponding GSB bands in the GA amplitude spectrum of the ≈150 fs component, which is representative of the TA spectrum of the doped chromophores, we find that a chromophore contains about 3.3 neutral monomers for 1 charged monomer with 600 nm excitation (Figure S6b, Supporting Information; Table 1). This drops to 1.9 neutral monomers per polaron with 1100 nm excitation, evidencing the reduced delocalization of the doped chromophores excited in the P_2 band.

In addition to the electronic coupling of the polaron to adjacent neutral sites, intersite Coulomb interactions can take place between the charged site and its surroundings in doped CPE-K. Such Coulomb shifts of the energy levels in doped organic systems have been theoretically predicted and experimentally observed by photoelectron spectroscopy in previous work.[18] Additionally, if the ground and excited states are affected by the field to different extents, this can cause a Stark shift of the optical transitions.[30] For CPE-K, the backbone of the polymer consists of alternating donor–acceptor units, so that a change in polarity and/or polarizability between the ground and excited state can be expected. Indeed, there is a 12 nm red-shift (from 691 to 703 nm) of the N_1 transition in the steady-state absorption spectra when going from undoped to doped CPE-K film, pointing to such an effect (Figure 1a). The electric field generated by the polarons thus shifts the N_1 transition of nearby undoped sites to the red (as shown in the schematics on the right of Figure 3d). In the TA spectra, the precise position of the N_1 GSB is difficult to quantify due to overlap with positive bands and more limited spectral resolution. Still, there is a clear red-shift of the N_1 GSB band in the 150 fs amplitude spectrum (of only doped chromophores), with 1100 nm (P_2) compared to 600 nm (N_1) excitation (left of Figure 3d, Table 1). Due to the reduced delocalization of the chromophores with P_2 excitation (see above), the neutral sites probed at 1100 nm are closer to the polaron and therefore feel a stronger electric field, explaining the increased red-shift. However, the amplitude spectra of the 2.5 ps decay component, which represent the undoped chromophores not coupling to a polaron, are similar at both excitation wavelengths. Here, the N_1 GSB is only slightly blue-shifted compared to the 150 fs amplitude spectrum at 600 nm excitation (Table 1), implying that the undoped chromophores are still affected by the charges (as confirmed below by solution measurements).

2.4. Excited State Dynamics in Doped CPE-K/H_2SO_4 Films

To investigate the effect of doping concentration, we performed TA measurements on heavily doped CPE-K/H_2SO_4 films. In Figure 1a, the higher doping concentration after addition of H_2SO_4 to CPE-K is obvious when comparing the ratio between the absorption bands for the N_1 and P_2 transitions, which clearly increases in CPE-K/H_2SO_4. We have shown above that the concentration of doped monomers increases from 17% to 27% with the addition of acid, as also confirmed via EPR and conductivity measurements.[3,11] The doping level is relatively high for both CPE-K and CPE-K/H_2SO_4 films, with practically all chains containing doped sites and being close to polarons of other chains due to chain packing in the films (insets of **Figure 4**a). The P_2 polaron absorption band is blue-shifted in CPE-K/H_2SO_4 (Table 1), which is attributed to Coulomb repulsion between adjacent positive polarons resulting in their destabilization (and suggesting a smaller distance between polarons in the heavily doped system).[31] The N_1 absorption band is however at a similar spectral position in doped and heavily doped CPE-K, showing that the Stark shift of the N_1 transition due to the electric field of the polarons is comparable at both doping levels. In the TA data for CPE-K/H_2SO_4 film, for both 600 and 1100 nm excitation at early times (0.1 ps), we observe the N_1 GSB and the NIR PA bands as in CPE-K (Figure 4a), as well as the P_2 GSB. The coupling between the N_1 and P_2 transitions thus persists in the highly doped system. For CPE-K/H_2SO_4, the N_1 GSB seems blue-shifted compared to its steady-state absorption, but this is mostly due to overlap with positive PA signatures on the red side of the band. Nevertheless, the red-shift of this band with P_2 excitation of less delocalized chromophores is still present (as for doped CPE-K, Table 1). Doped CPE-K and heavily doped CPE-K/H_2SO_4 films decay with similar time constants (inset of Figure 4b). This is confirmed by the GA results for CPE-K/H_2SO_4 for excitation of the N_1 transition at 600 nm (Figure 4b) and at 1100 nm (Figure S7, Supporting Information) that show recombination of doped chromophores with the 150 fs time constant and of undoped chromophores with the 2.5 ps time constant (and weak offset).

Comparing the amplitudes of the decay components (Table 1), we find that 81% of neutral monomers couple to polarons in CPE-K/H_2SO_4 with 600 nm excitation, which is similar to doped CPE-K (83%). The weight of the undoped chromophores thus remains the same at both doping levels, implying that their coupling to polarons is likely disrupted by chemical or conformational defects, independently of the doping concentration. In the early TA spectra (Figure 4a) and 150 fs amplitude spectra (Figure S6b, Supporting Information), it can be seen that with 600 nm excitation, the P_2 GSB is more pronounced in the heavily doped system than in less doped CPE-K, while the N_1 GSB has similar intensity (as expected for the same excitation density). From the ratio of the two bands

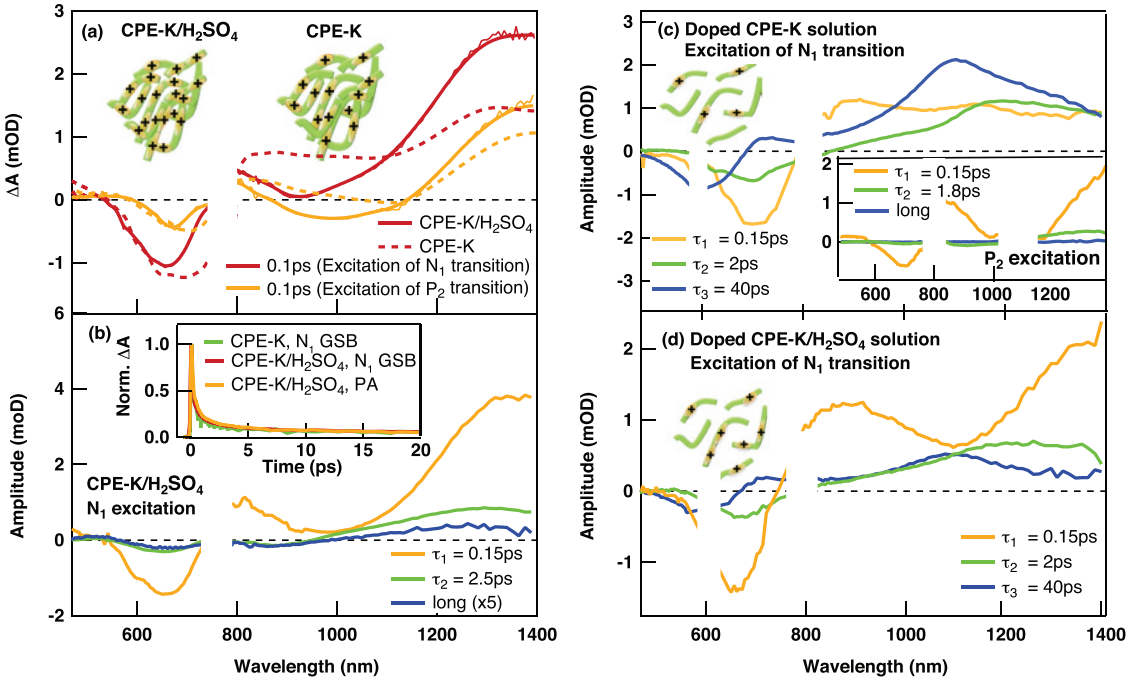

Figure 4. Transient absorption (TA) results for films and solutions of doped CPE-K and CPE-K/H_2SO_4 with different doping concentrations. a) TA spectra at an early time delay (0.1 ps) following photoexcitation at 600 and 1100 nm at an absorbed photon density of ≈1.5×10^{13} cm^{-2} for films of heavily doped CPE-K/H_2SO_4 (solid lines) and doped CPE-K (dashed lines). In the inset, a simplified scheme of the doped conjugated polymer chains in CPE-K/H_2SO_4 and CPE-K films is shown. b) Amplitude spectra associated with the different recombination time constants (0.15, 2.5 ps, long-lived offset) as derived from the multiexponential global analysis of the TA data for CPE-K/H_2SO_4 film with 600 nm excitation at an absorbed photon density of ≈1.5×10^{13} cm^{-2}. In the inset, the normalized dynamics for CPE-K/H_2SO_4 and CPE-K via 600 nm excitation are compared, probed either at the N_1 GSB (visible ground state bleaching) or PA (photoinduced absorption) band maxima. Amplitude spectra for c) doped CPE-K solution and d) heavily doped CPE-K/H_2SO_4 solution, obtained by multiexponential global analysis (time constants of 0.15, 2, and 40 ps) of the TA data obtained with 600 nm excitation (scaled to be equivalent to an absorbed photon density of ≈1.5×10^{13} cm^{-2}). In the insets, a simplified scheme of the doped conjugated polymer chains in solution is shown. The inset of c) depicts moreover the amplitude spectra obtained by multiexponential global analysis of the TA data for doped CPE-K solution via 1100 nm excitation (time constants of 0.15, 1.8 ps, and offset).

in the 150 fs amplitude spectrum, we find that the doped chromophores are more localized in CPE-K/H_2SO_4, containing 2.3 (instead of 3.3) neutral monomers per doped one (Table 1). We attribute this to the smaller number of neutral monomers available between doped sites in the heavily doped chains, due to the higher doping concentration and smaller distance between polarons. The 2.3:1 neutral to polaron ratio in the doped chromophores is consistent with the overall 27% doping level (from the steady-state absorption, Table 1), which means that per doped monomer there are in total 2.7 neutral ones, from which we saw that about 81% couple to a polaron (undergoing recombination in 150 fs). Another possible explanation for the more pronounced P_2 GSB would be excitation of the tail of the strongly blue-shifted P_2 band of CPE-K/H_2SO_4 film at 600 nm (Figure 1a). Given the excellent match of the doped chromophore delocalization with the available number of monomers, this is however not expected to play a significant role. Finally, with P_2 excitation at 1100 nm, the ratio between the N_1 GSB and P_2 GSB is similar for doped CPE-K and CPE-K/H_2SO_4 (1.8–1.9 neutral monomers per charge, Table 1), showing that the delocalization of the chromophores is in this case purely electronically defined. Overall, we show that most neutral sites are affected similarly by the polarons in both doped CPE-K and heavily doped CPE-K/H_2SO_4 films and experience a similar electronic environment independently of the doping concentration.

2.5. Doped CPE-K and CPE-K/H_2SO_4 Solutions

To remove the effects of intermolecular interactions and to access lower doping levels, we have dissolved doped CPE-K and heavily doped CPE-K/H_2SO_4 in solution. Some de-doping occurs during dissolution, so that the polaron concentration is lower in the solutions than in the corresponding films. From the absorption spectra (Figure 1a; Figure S2, Supporting Information), we have found that 8% and 14% of monomers are charged in doped CPE-K and CPE-K/H_2SO_4 solution, respectively, compared to 17% and 27% in the corresponding films. At the lower doping concentrations of the solutions, we expect that some CPE-K chains are entirely undoped and also isolated from other doped chains when dissolved (inset of Figure 4c). Due to various environmental effects (absence of packing, lower polaron concentration, solvation), the N_1 band in the solutions is blue-shifted to 650 nm (doped CPE-K) and to 667 nm (doped CPE-K/H_2SO_4) compared to the films (703 nm for both, Table 1). We will show that the more red-shifted N_1 transition in CPE-K/H_2SO_4 is caused by a higher number of doped chains

feeling the electric field of the polarons. The P_2 band is on the other hand at slightly higher wavelength than in the films, at 1150 nm (vs 1120 nm) in doped CPE-K and at 1080 nm (vs 950 nm) in CPE-K/H_2SO_4. The blue-shift in the more heavily doped system, due to closer proximity between polarons, thus persists to a lesser extent in solution.

Because of the presence of entirely undoped as well as doped CPE-K chains in the solutions, the TA spectra with 600 nm excitation (Figure S8, Supporting Information) appear quite different from the corresponding ones recorded in films, where we have estimated that all polymer chains contain at least one polaron. In the GA results for dissolved doped CPE-K (Figure 4c) and CPE-K/H_2SO_4 (Figure 4d) with 600 nm excitation, we observe that the N_1 GSB of the solutions is an overlap of blue- and red-shifted bands that recombine with different rates. The ultrafast ≈150 fs component due to recombination in doped chromophores is still present, evidencing that the coupling of the N_1 and P_2 transitions is maintained for the doped chains in solution. The position of the N_1 GSB in the 150 fs amplitude spectra is similar as in the films (at ≈700 nm for doped CPE-K, Table 1), which is strongly red-shifted compared to the steady-state solution spectra and shows a strong Stark shift in the doped chains (Table 1). A recombination component of 2 ps is seen in the doped CPE-K and CPE-K/H_2SO_4 solutions, which is also comparable to what is observed in the corresponding films in terms of the time constant and red-shifted position of the N_1 GSB (Figure 4c,d). We assign this to undoped chromophores located on chains containing a polaron, thus feeling its electric field but not coupling to it. Comparing the weight of the N_1 GSB of only the 150 fs and 2 ps components in the solutions (which discards the effect of the entirely undoped chains), we find that 71% (CPE-K) and 80% (CPE-K/H_2SO_4) of the monomers on the doped chains couple to polarons, which is only slightly lower than in the films (Table 1). In contrast, the blue-shifted N_1 GSB in the doped CPE-K and CPE-K/H_2SO_4 solutions is located at 600 nm (over 100 nm shift compared to the doped chromophores, Table 1). It recombines more slowly (≈40 ps) and is related to a NIR PA band peaking at ≈1150 nm (Figure 4c,d). It is attributed to isolated undoped CPE-K chains, that are not affected in any way by the polarons and do not show any Stark effect. As expected, this pronounced slow decay component is absent in films and is weaker in the more doped solution (where more chains contain a polaron). From the amplitude of the N_1 GSB of the 40 ps component (undoped chains) compared to the ones of the two faster time constants (doped chains), we estimate that about 28% of the chains are entirely undoped in the CPE-K solution, which drops to 14% in the CPE-K/H_2SO_4 solution (Table 1). Since the steady-state absorption spectra are the sum of doped and undoped chains, the N_1 band is found at a spectral position that corresponds to their weighted average, which is thus more red-shifted in CPE-K/H_2SO_4.

From the ratio of the N_1 GSB to P_2 GSB in the 150 fs amplitude spectrum of doped CPE-K solution with 600 nm excitation (Figure S6b, Supporting Information; Table 1), we find that for every charged monomer in a doped chromophore, there are 3.2 neutral ones in doped CPE-K solution, which is very similar to the value of 3.3 found in the corresponding film. We therefore evidence a similar delocalization of the doped chromophores in film and solution, showing that the coupling of the N_1 and P_2 transitions is essentially intrachain and does not depend on chain packing. This is likely the intrinsic electronic delocalization of doped chromophores excited at 600 nm, which is not limited by the available number of neutral monomers. On the other hand, in CPE-K/H_2SO_4 solution, the ratio of neutral to charged monomers in the doped chromophores drops to 2.6:1 (Table 1), consistent with the reduced distance between polarons causing the blue-shift in the absorption. As expected at the lower doping level in solution, the effect is less pronounced than in the corresponding film (2.3 neutral monomers per polaron). Finally, with 1100 nm excitation of the P_2 transition of the doped CPE-K and CPE-K/H_2SO_4 solutions, the doped chromophores are selectively excited, so that only the red-shifted N_1 GSB is observed (inset of Figure 4c; Figure S9, Supporting Information). There are no longer any effects due to the undoped chains, therefore the TA spectra and dynamics are essentially the same as in the corresponding films (Figures S9 and S10, Supporting Information). The GA amplitude spectra are dominated by the 150 fs decay of the doped chromophores (which contain 1.7–1.8 neutral monomers per charge, showing similar delocalization between the two doping levels and with the films, Table 1). The very weak slower components (1.8 ps and offset) are again due to residual population of undoped chromophores on the doped chains. We thus evidence a dual behavior of independent doped and undoped CPE-K chains in solution, allowing an even more direct comparison of their properties. The doped polymer chains in solution show the same characteristic coupling of the N_1 and P_2 transitions, ultrashort excited state lifetime and Stark-shifted N_1 GSB as was discussed in films, while the undoped chains show no effect of the polarons.

2.6. Jablonski Diagram of Doped CPE-K

Based on our results, we propose a Jablonski state diagram that describes the doped CPE-K system, as depicted in **Figure 5**, including electronic transitions that take place via photoexcitation (solid arrows) and recombination processes (dashed arrows). We stipulate that a CPE-K polymer chain does not act as a single chromophore but breaks into doped und undoped segments. In the doped chromophores, the neutral sites are close to a polaron and strongly electronically couple to it, implying delocalization of the electronic states over the entire segment including its polaronic and neutral monomers. In the undoped chromophores, the neutral sites are located further away from the polarons (not coupling to it) or their conjugation to the polarons is disrupted by conformational or chemical defects, but they can still feel the electric field of the polarons if they are located on the same chain.

In general, due to disorder and coupling to nuclear modes, optical absorption in conjugated polymers occurs within a chromophoric segment and not over the entire conjugated backbone.[8,32,33] Electronic relaxation and self-trapping processes then further localize the initially excited state on the subpicosecond time scale. By considering exciton–exciton annihilation occurring at high excitation densities faster than our ≈70 fs experimental time resolution, we estimate that initially

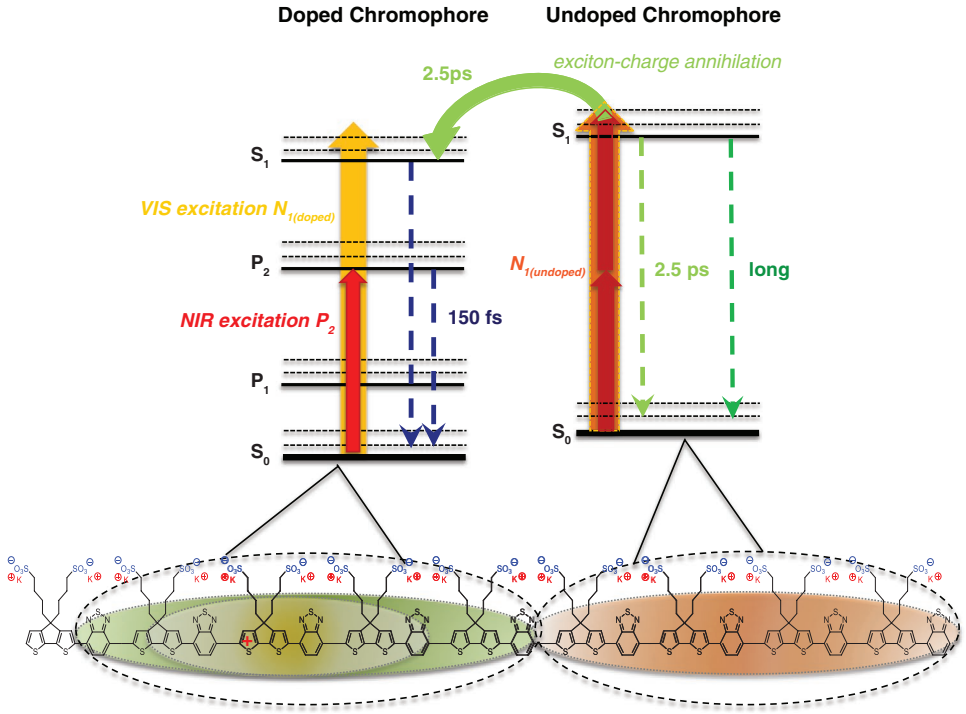

Figure 5. Jablonski diagram illustrating the electronic states in doped CPE-K. The electronic transitions via visible (N_1) and near-infrared (P_2) excitation are indicated with solid arrows and recombination processes with dashed arrows. On the left, the states of doped chromophores (containing a polaronic site) are shown and on the right, the states of undoped chromophores. On the bottom, a schematic representation of chains in doped CPE-K including doped photoexcited chromophores (green and yellow shaded ovals, depending on N_1 or P_2 excitation, respectively) and undoped photoexcited chromophores (dark orange shaded oval) are depicted. Strong electronic coupling between polarons and nearby neutral sites on the backbone of the conjugated polyelectrolyte is demonstrated. In addition, Coulomb interactions between doped and nearby neutral sites affect the energy levels of the latter.

photoexcited segments in undoped CPE-K film span ≈4 nm (with 600 nm excitation), which corresponds to ≈3–4 monomers (using a monomer size of ≈1.2 nm,[34] Figure S11, Supporting Information). This agrees with the wavefunction delocalization (≈4–5 monomers) obtained for PCPDTBT via theoretical DFT calculations.[25] Therefore, it can indeed be expected that the backbone of doped CPE-K breaks into several chromophoric segments, even for relatively short CPE-K chains of 7–14 monomers as the ones used here. The existence of doped and undoped chromophores is thus justified (green and orange ovals in Figure 5), as well as the size of ≈3 monomers that we find when analyzing the delocalization of the doped chromophores based on the ratio of the N_1 and P_2 GSB bands in the TA data (Table 1).

In both doped CPE-K and heavily doped CPE-K/H_2SO_4 films, we find the excited state dynamics to be strongly dominated by the doped segments, given the relatively high doping levels where each polymer chain contains at least 1–2 polaronic sites. When exciting the N_1 transition at 600 nm, both the doped and undoped chromophores are photoexcited (with about 80% and 20% weight, respectively), and absorb via the $N_{1(doped)}$ and $N_{1(undoped)}$ transitions, as shown in Figure 5. Our TA results unambiguously establish that the neutral sites in the doped chromophores strongly couple to the polaronic sites in spite of the structural distortion of the polaron. The $N_{1(doped)}$ transition thus leads to the simultaneous appearance of the N_1 and P_2 GSB bands in our TA data, and to a predominant ultrafast (≈150 fs) recombination component. As shown on the left of the Jablonski diagram in Figure 5, the coupling of the neutral and polaronic sites on the same doped chromophore implies that the lower excited states of the segment are the ones populated by the P_2 and P_1 transitions. Therefore, the S_1 state can decay nonradiatively via internal conversion to the low-lying polaronic states, which are known to have very short lifetimes.[29] We note that the ratio of the N_1 GSB to P_2 GSB in the 150 fs amplitude spectrum allows to estimate the delocalization of the doped chromophores to 3.3 neutral monomers (in doped CPE-K) and to 2.3 neutral monomers (in heavily doped CPE-K/H_2SO_4) per charged site, the smaller chromophore size in the latter likely being due to less available neutral sites between the polarons. In solution, the doping level drops and entirely undoped isolated polymer chains are present (28% and 14% in CPE-K and CPE-K/H_2SO_4, respectively). The properties of the remaining doped chains are nevertheless quite similar as in the films, in terms of doped chromophore delocalization and position of the N_1 absorption band. This N_1 transition (for both doped and undoped chromophores) is red-shifted whenever a polaron is present on the chain, due to the Stark effect caused by the electric field around the charge.

The doped chromophores of CPE-K and CPE-K/H_2SO_4 in films and solutions are more selectively excited at 1100 nm of the P_2 transition (red arrow in Figure 5), leading to a similar excited state behavior as with $N_{1(doped)}$ excitation at 600 nm, that is characterized by the simultaneous N_1 and P_2 GSB signatures

and an ultrafast 150 fs decay. The P_2 GSB is in this case more pronounced compared to the N_1 GSB, due to a smaller delocalization of the doped chromophores excited at 1100 nm (yellow oval in Figure 5). We find 1.7–1.9 neutral monomers per charged monomer at both doping levels and in both films and solutions. Indeed, it has been reported from theoretical calculations and polarization-sensitive measurements on conjugated polymers, that a lower excitation energy leads to less delocalized initially excited electronic states.[8,33,35] Targeted excitation of the doped chromophores at 1100 nm also allows to evidence a slightly red-shifted N_1 GSB, since the probed neutral sites are closer to the polaron due to the reduced delocalization, and thus feel a stronger Coulomb potential.

Finally, for all investigated doped samples in films and solutions, we observe a slower excited state decay component (1.8–2.5 ps), mainly with 600 nm excitation and to a lesser extent with 1100 nm excitation. We assign this to recombination in undoped segments (right side of the Jablonski diagram in Figure 5). The N_1 GSB of the corresponding amplitude spectrum is at a similar position as seen in the doped chromophores, showing that the undoped segments are still located on doped polymer chains and feel the electric field of the charge. They are either directly excited via the $N_{1(undoped)}$ transition at 600 nm (dark orange arrow), populated when some initially excited doped chromophores localize on neutral sites during ultrafast excited state relaxation, or excited by residual two-photon absorption (double dark red arrows). Since the low-lying polaronic states are absent on the undoped segments, their recombination is slower (green dashed arrows). The slower decay components are assigned to nonradiative recombination of undoped chromophores similar as seen in undoped CPE-K film (Figure S3, Supporting Information) and/or to exciton-polaron annihilation, which is an incoherent recombination mechanism that involves Förster energy transfer from the undoped segment to the polaronic site.[26,28] This can occur due to the proximity of the undoped and doped chromophores on the same doped polymer chain, in both films and solutions. However, entirely undoped and isolated chains exist only in solution, and they are characterized by even slower decay dynamics (40 ps component) and a strongly blue-shifted N_1 GSB (by about 100 nm).

3. Conclusion

In summary, we have presented here the first in-depth study of the ultrafast photophysics of a self-doped conjugated polyelectrolyte, highlighting the optoelectronic properties of doping-induced polarons and their interactions with their surroundings. We chose a cationic self-doped system, which presents particularly high advantages in terms of stability (no dopant diffusion), similar morphology compared to the undoped film,[12] and absence of intermolecular orbital hybridization with the dopant. Our most important finding is that there is strong electronic coupling of the polaronic site to nearby neutral sites, which share the same ground state for their optical transitions. This is unambiguously demonstrated by the simultaneous depletion of both the neutral and polaronic transitions, as well as by correlated excited state dynamics, when either transition is photoexcited during femtosecond transient absorption experiments. This result contrasts with the conventional picture of localized intragap polaron states and agrees with a revised model for the electronic structure and optical transitions in doped organic systems.[5,17–19] Second, our study shows that intersite Coulomb interactions are present, so that the positive polarons cause a Stark shift in the transitions of nearby neutral sites. The electronic coupling and electrostatic effects of the polarons occur independently on doping concentration and both in thin films or in solution.

Achieving high conductivity in doped organic semiconductors requires high mobility and a high yield of free charges that do not remain bound (electrostatically or by orbital hybridization) to the ionized dopant.[3,5,6c] Here, via spectroscopic elucidation of the optoelectronic properties of a self-doped system, we find characteristics of the polaron that might help its dissociation from interfacial bound states. In particular, we show that the polaron delocalizes across neighboring neutral sites along the conjugated backbone, and also couples into their frontier energy levels, which are the ones responsible for charge transport.[36] We thus demonstrate an electronic connectivity of the polarons to their local surroundings, which likely helps the polarons to become mobile and to separate from their charged counterion. In analogy, nanoscale charge transport has also been identified as a key factor in the charge separation of photogenerated polarons in organic solar cell blends.[37] The importance of polaron delocalization in doped conjugated polymers for high hole mobilities has also been demonstrated by early work on conjugated polymers doped with small molecules such as iodide, where the optical properties of polarons in doped polymers with different interchain interactions were studied.[24] We conclude that it is essential to develop useful predictive models of not only the electrical and transport characteristics, but also of the optoelectronic properties of the polarons on the conjugated backbone. Our findings bring significant new insights to doped organic systems, since we provide evidence of polaron delocalization to neighboring neutral sites that can ultimately increase the conductivity and macroscopic mobility upon doping.[38]

4. Experimental Section

Sample Preparation: For this work, CPE-K was studied in solution and as thin films. Details for the synthesis are reported elsewhere.[10,23] For making films, CPE-K solutions were prepared by first dissolving CPE-K into water of resistivity = 18.2 Ω cm, sonicating until all the material was dissolved, then adding MeOH to give a 20 mg mL^{-1} solution of CPE-K in H_2O/MeOH (3:2). The solution was filtered through a 0.45 µm PTFE syringe filter prior to use. To prepare CPE-K/H_2SO_4 and undoped CPE-K solutions, one molar equivalent of respectively H_2SO_4 or KOH per monomer unit of CPE-K was added to the CPE-K solution. The quartz substrates were cleaned in a sonicator with soapy water, water, acetone, and isopropanol for 15 min each, blow dried using N_2, and further treated with UV–ozone for 1 h. Thin films of CPE-K were prepared by spin casting 100 µL of the different CPE-K solutions onto the aforementioned quartz substrates. The spin coating parameters were 1000 rpm for 30 s followed by 5000 rpm for 30 s. Film thickness measurements were performed using an Ambios XP-100 stylus profilometer. A line was scored on each sample in order to measure the thickness. In order to prepare CPE-K and CPE-K/H_2SO_4 in solution for absorption and TA experiments, the polymers were re-dissolved in H_2O/MeOH (1:1) under

nitrogen atmosphere and the resulting solutions were diluted to have an absorbance of ≈0.18–0.21 at 600 nm (≈42–49 µg mL^{-1}). The absorption spectra of the films and solutions were measured with a Lambda 950 UV–vis–IR spectrophotometer (Perkin Elmer).

Transient Absorption Spectroscopy: To study the excited state dynamics, spectrally resolved femtosecond TA measurements were performed using a Ti:Sapphire amplifier system (Astrella, Coherent). The output pulses had a time duration of ≈35 fs, 800 nm center wavelength, repetition rate of 1 kHz and energy of ≈6 mJ per pulse. Part of the amplifier output was used to pump the optical parametric amplifier (OPA) (Opera, Coherent) that converted the photon energy of the incident beam to the wavelength used to photoexcite the samples. Pump wavelengths at 600 and 1100 nm were used. Probe wavelengths covering the visible and near-infrared region ranging from 480 to 1300 nm were spectrally resolved. This was achieved via continuum white light pulses generated by strongly focusing a small part of the fundamental beam onto a 5 mm sapphire plate. Part of the probe pulses were then temporally and spatially overlapped on the sample with the pump pulses, while the other part was used as a reference. The transmitted probe beam through the sample and the reference beam were spectrally dispersed in two home-built prism spectrometers (Entwicklungsbüro Stresing, Berlin) and detected separately with either back-thinned Silicon CCDs (Hamamatsu S07030-0906) or InGaAs arrays (Hamamatsu) for, respectively, visible and near-infrared detection. The transmission change of the probe pulses following photoexcitation was recorded for different pump-probe time delays up to nanoseconds, while the pump pulses were chopped at 500 Hz for the signal to be measured shot by shot. The TA changes induced by the pump were monitored with 70 fs time resolution. The beam sizes of the excitation and probe pulses were ≈1 mm and 250 µm, respectively to ensure uniform distribution of detected photoexcited species. To avoid anisotropy effects, the relative polarization of the probe and pump pulses was set at the magic angle. The TA spectra for the entire time window were scanned multiple times for both films and solutions without any significant signs of degradation. For solid state measurements the films were sealed in a chamber filled with nitrogen, while the solutions were placed in a quartz cuvette with an optical path length of 2 mm (Starna Cells Inc.). All TA data was corrected for the chirp of the white light.

Multi-Exponential Global Analysis: To distinguish between overlapping spectral features corresponding to different photoexcited species and processes, multiexponential GA was used. In this procedure, the entire spectral and temporal pump-probe data sets were analyzed simultaneously using the sum of exponential functions. This involved analyzing the time profiles at all probe wavelengths using the same time constants but allowing the pre-exponential amplitudes to vary freely. For all systems studied here, a bi-exponential function and an offset, which represents species that live longer than the 1 ns time window of the measurement, were used. An additional term was added that convolutes with the bi-exponential function to include the instrument-response-limited rise of the TA signal at early times. This is described by a Gaussian function where the full-width-at-half-maximum is related to the temporal resolution of the experiment (70–80 fs). The GA approach yields the amplitude spectra with their associated time constants for different relaxation and recombination processes that influence the overall TA signal at different timescales, facilitating the interpretation of the dynamics.

Supporting Information

Supporting Information is available from the Wiley Online Library or from the author.

Acknowledgements

D.T., L.P., and N.B. thank the European Research Council (ERC) for supporting this research by a Starting Grant (No. 714586, OSIRIS), and acknowledge NCCR-MUST, a research instrument of the Swiss National Science Foundation, as well as the University of Bern. D.X.C. acknowledges the support by the National Science Foundation Graduate Research Fellowship Program under Grant No. 1650114. Any opinions, findings, and conclusions, or recommendations expressed in this material are those of the authors and do not necessarily reflect the views of the National Science Foundation. C.-K. M., G. C. B., and T.-Q. N. thank the Institute of Collaborative Biotechnologies under Grant No. W911F-09-D-0001 from the U.S. Army Research Office.

Conflict of Interest

The authors declare no conflict of interest.

Keywords

cationic polarons, doping in conjugated polymers, excited state dynamics

Received: July 29, 2019
Revised: November 15, 2019
Published online:

[1] a) B. Lüssem, M. Riede, K. Leo, *Phys. Status Solidi A* **2013**, *210*, 9; b) X. Zhao, X. Zhan, *Chem. Soc. Rev.* **2011**, *40*, 3728.
[2] Q. Cui, G. C. Bazan, *Acc. Chem. Res.* **2018**, *51*, 202.
[3] C. Gaul, S. Hutsch, M. Schwarze, K. S. Schellhammer, F. Bussolotti, S. Kera, G. Cuniberti, K. Leo, F. Ortmann, *Nat. Mater.* **2018**, *17*, 439.
[4] a) I. E. Jacobs, A. J. Moulé, *Adv. Mater.* **2017**, *29*, 1703063; b) B. Lüssem, C.-M. Keum, D. Kasemann, B. Naab, Z. Bao, K. Leo, *Chem. Rev.* **2016**, *116*, 13714; c) K. Kang, S. Watanabe, K. Broch, A. Sepe, A. Brown, I. Nasrallah, M. Nikolka, Z. Fei, M. Heeney, D. Matsumoto, K. Marumoto, H. Tanaka, S.-i. Kuroda, H. Sirringhaus, *Nat. Mater.* **2016**, *15*, 896; d) Y. Hu, Z. D. Rengert, C. McDowell, M. J. Ford, M. Wang, A. Karki, A. T. Lill, G. C. Bazan, T.-Q. Nguyen, *ACS Nano* **2018**, *12*, 3938.
[5] I. Salzmann, G. Heimel, M. Oehzelt, S. Winkler, N. Koch, *Acc. Chem. Res.* **2016**, *49*, 370.
[6] a) P. Pingel, D. Neher, *Phys. Rev. B* **2013**, *87*, 115209; b) A. Mityashin, Y. Olivier, T. Van Regemorter, C. Rolin, S. Verlaak, N. G. Martinelli, D. Beljonne, J. Cornil, J. Genoe, P. Heremans, *Adv. Mater.* **2012**, *24*, 1535; c) M. L. Tietze, J. Benduhn, P. Pahner, B. Nell, M. Schwarze, H. Kleemann, M. Krammer, K. Zojer, K. Vandewal, K. Leo, *Nat. Commun.* **2018**, *9*, 1182.
[7] a) J. C. Brauer, M. Causa, N. Banerji, *Nanostructured Materials for Type III Photovoltaics*, The Royal Society of Chemistry, London, UK **2018**, p. 226; b) I. A. Howard, R. Mauer, M. Meister, F. Laquai, *J. Am. Chem. Soc.* **2010**, *132*, 14866; c) T. M. Clarke, J. R. Durrant, *Chem. Rev.* **2010**, *110*, 6736.
[8] N. Banerji, *J. Mater. Chem. C* **2013**, *1*, 3052.
[9] a) C. V. Hoven, A. Garcia, G. C. Bazan, T.-Q. Nguyen, *Adv. Mater.* **2008**, *20*, 3793; b) F. Huang, H. Wu, Y. Cao, *Chem. Soc. Rev.* **2010**, *39*, 2500; c) A. Duarte, K.-Y. Pu, B. Liu, G. C. Bazan, *Chem. Mater.* **2011**, *23*, 501; d) H. Jiang, P. Taranekar, J. R. Reynolds, K. S. Schanze, *Angew. Chem., Int. Ed.* **2009**, *48*, 4300; e) K. Y. Pu, B. Liu, *Adv. Funct. Mater.* **2011**, *21*, 3408.
[10] C.-K. Mai, R. A. Schlitz, G. M. Su, D. Spitzer, X. Wang, S. L. Fronk, D. G. Cahill, M. L. Chabinyc, G. C. Bazan, *J. Am. Chem. Soc.* **2014**, *136*, 13478.
[11] C.-K. Mai, H. Zhou, Y. Zhang, Z. B. Henson, T.-Q. Nguyen, A. J. Heeger, G. C. Bazan, *Angew. Chem., Int. Ed.* **2013**, *52*, 12874.

[12] H. Zhou, Y. Zhang, C.-K. Mai, S. D. Collins, T.-Q. Nguyen, G. C. Bazan, A. J. Heeger, *Adv. Mater.* **2014**, *26*, 780.
[13] a) H. Zhou, Y. Zhang, C.-K. Mai, J. Seifter, T.-Q. Nguyen, G. C. Bazan, A. J. Heeger, *ACS Nano* **2015**, *9*, 371; b) H. Choi, C.-K. Mai, H.-B. Kim, J. Jeong, S. Song, G. C. Bazan, J. Y. Kim, A. J. Heeger, *Nat. Commun.* **2015**, *6*, 7348.
[14] a) G. Parthasarathy, C. Shen, A. Kahn, S. R. Forrest, *J. Appl. Phys.* **2001**, *89*, 4986; b) J. Niklas, K. L. Mardis, B. P. Banks, G. M. Grooms, A. Sperlich, V. Dyakonov, S. Beaupré, M. Leclerc, T. Xu, L. Yu, O. G. Poluektov, *Phys. Chem. Chem. Phys.* **2013**, *15*, 9562.
[15] a) D. T. Duong, H. Phan, D. Hanifi, P. S. Jo, T. Q. Nguyen, A. Salleo, *Adv. Mater.* **2014**, *26*, 6069; b) H. Kleemann, C. Schuenemann, A. A. Zakhidov, M. Riede, B. Lüssem, K. Leo, *Org. Electron.* **2012**, *13*, 58.
[16] a) H. Méndez, G. Heimel, S. Winkler, J. Frisch, A. Opitz, K. Sauer, B. Wegner, M. Oehzelt, C. Röthel, S. Duhm, *Nat. Commun.* **2015**, *6*, 8560; b) D. Di Nuzzo, C. Fontanesi, R. Jones, S. Allard, I. Dumsch, U. Scherf, E. Von Hauff, S. Schumacher, E. Da Como, *Nat. Commun.* **2015**, *6*, 6460.
[17] G. Heimel, *ACS Cent. Sci.* **2016**, *2*, 309.
[18] S. Winkler, P. Amsalem, J. Frisch, M. Oehzelt, G. Heimel, N. Koch, *Mater. Horiz.* **2015**, *2*, 427.
[19] R.-Q. Png, M. C. Ang, M.-H. Teo, K.-K. Choo, C. G. Tang, D. Belaineh, L.-L. Chua, P. K. Ho, *Nat. Commun.* **2016**, *7*, 11948.
[20] a) J. L. Bredas, G. B. Street, *Acc. Chem. Res.* **1985**, *18*, 309; b) J. Brédas, F. Wudl, A. Heeger, *Solid State Commun.* **1987**, *63*, 577.
[21] D. Campbell, A. Bishop, K. Fesser, *Phys. Rev. B* **1982**, *26*, 6862.
[22] M. C. Scharber, M. Koppe, J. Gao, F. Cordella, M. A. Loi, P. Denk, M. Morana, H. J. Egelhaaf, K. Forberich, G. Dennler, *Adv. Mater.* **2010**, *22*, 367.
[23] D. Cao, D. Leifert, V. V. Brus, M. S. Wong, H. Phan, B. Yurash, N. Koch, G. C. Bazan, T.-Q. Nguyen, unpublished.
[24] R. Österbacka, C. P. An, X. Jiang, Z. V. Vardeny, *Science* **2000**, *287*, 839.
[25] R. Tautz, E. Da Como, C. Wiebeler, G. Soavi, I. Dumsch, N. Fröhlich, G. Grancini, S. Allard, U. Scherf, G. Cerullo, *J. Am. Chem. Soc.* **2013**, *135*, 4282.
[26] a) F. Montilla, A. Ruseckas, I. D. Samuel, *J. Phys. Chem. C* **2018**, *122*, 9766; b) S. van Reenen, M. Vitorino, S. Meskers, R. Janssen, M. Kemerink, *Phys. Rev. B* **2014**, *89*, 205206.
[27] T. Q. Nguyen, I. B. Martini, J. Liu, B. J. Schwartz, *J. Phys. Chem. B* **2000**, *104*, 237.
[28] J. M. Hodgkiss, S. Albert-Seifried, A. Rao, A. J. Barker, A. R. Campbell, R. A. Marsh, R. H. Friend, *Adv. Funct. Mater.* **2012**, *22*, 1567.
[29] A. A. Bakulin, A. Rao, V. G. Pavelyev, P. H. M. van Loosdrecht, M. S. Pshenichnikov, D. Niedzialek, J. Cornil, D. Beljonne, R. H. Friend, *Science* **2012**, *335*, 1340.
[30] L. Sebastian, G. Weiser, H. Bässler, *Chem. Phys.* **1981**, *61*, 125.
[31] a) N. Takeda, S. Asaoka, J. R. Miller, *J. Am. Chem. Soc.* **2006**, *128*, 16073; b) L. Zaikowski, P. Kaur, C. Gelfond, E. Selvaggio, S. Asaoka, Q. Wu, H.-C. Chen, N. Takeda, A. R. Cook, A. Yang, *J. Am. Chem. Soc.* **2012**, *134*, 10852.
[32] T. E. Dykstra, E. Hennebicq, D. Beljonne, J. Gierschner, G. Claudio, E. R. Bittner, J. Knoester, G. D. Scholes, *J. Phys. Chem. B* **2009**, *113*, 656.
[33] O. R. Tozer, W. Barford, *J. Phys. Chem. A* **2012**, *116*, 10310.
[34] S. P. Danielsen, G. E. Sanoja, S. R. McCuskey, B. Hammouda, G. C. Bazan, G. H. Fredrickson, R. A. Segalman, *Chem. Mater.* **2018**, *30*, 1417.
[35] N. Banerji, S. Cowan, E. Vauthey, A. J. Heeger, *J. Phys. Chem. C* **2011**, *115*, 9726.
[36] H. Bässler, A. Köhler, *Unimolecular and Supramolecular Electronics I*, Vol. *312* (Ed: R. M. Metzger), Springer, Berlin Heidelberg **2012**, p. 1.
[37] T. M. Burke, M. D. McGehee, *Adv. Mater.* **2014**, *26*, 1923.
[38] a) R. Ghosh, C. M. Pochas, F. C. Spano, *J. Phys. Chem. C* **2016**, *120*, 11394; b) J.-F. Chang, H. Sirringhaus, M. Giles, M. Heeney, I. McCulloch, *Phys. Rev. B* **2007**, *76*, 205204.

